

Multi-reference Computational Method for De-novo Design, Optimization, and Repositioning of Pharmaceutical Compounds Illustrated by Identifying Multi-target SARS-CoV-2 Ligands

Vadim Alexandrov

Liquid Algo LLC <https://orcid.org/0000-0002-0254-9799>

Alexander Kirpich

Georgia State University <https://orcid.org/0000-0001-5486-0338>

Yuriy Gankin (✉ yuriy.gankin@quantori.com)

Quantori <https://orcid.org/0000-0003-0046-1037>

Research Article

Keywords: conformers, multi-reference, poly-conformational, in silico, ligand-based, structure-based, SARS COV-2, COVID-19, fingerprints, cheminformatics, similarity, virtual library, computational framework, validation

Posted Date: September 3rd, 2021

DOI: <https://doi.org/10.21203/rs.3.rs-153954/v2>

License: © ⓘ This work is licensed under a Creative Commons Attribution 4.0 International License.

[Read Full License](#)



Dear Journal of Cheminformatics Editorial Team,

We appreciate your consideration of our manuscript entitled “Multi-reference computational method for de-novo design, optimization, and repositioning of pharmaceutical compounds illustrated by identifying multi-target SARS-CoV-2 ligands”.

In this paper, we have proposed the multi-reference optimization approach in various in-silico drug discovery settings and illustrated its application and usefulness. We have also performed the validation of our approach for SARS-CoV-2 compounds and the corresponding results have been included in our manuscript. According to the proposed approach, each molecule is represented as an ensemble of flexible conformers that would choose the best possible conformation for each presented target-binding opportunity that can be applied in multiple settings. The aims were: a) to present a universal search framework for potential candidate compounds based on the comparison of multiple similarities between compounds’ conformers and b) to identify candidate compounds that are simultaneously similar to each of the selected known reference compounds. Application of this approach to SARS-CoV-2 produced several antiviral drug candidates that are designed to protect against SARS-CoV-2 by multiple mechanisms simultaneously.

Since this is a time sensitive matter, we appreciate your expedited consideration and review of our manuscript for publication in the Journal of Cheminformatics. Please do not hesitate to contact me with any additional inquiries regarding this submission.

On behalf of all authors,

Yuriy Gankin, Ph.D., MBA

Quantori. Custom Software Solutions.

625 Massachusetts Avenue

Cambridge, MA 02139

United States

E-mail: yuriy.gankin@quantori.com

Phone: (781) 771-1978

1 **Multi-reference computational method for de-novo design, optimization, and**
2 **repositioning of pharmaceutical compounds illustrated by identifying multi-**
3 **target SARS-CoV-2 ligands**

4

5

6

7 **Vadim Alexandrov¹, Alexander Kirpich² and Yuriy Gankin*³**

8

9 **1 Liquid Algo LLC, 85 Thistle Lane, Hopewell Junction, NY 12533, United States of America**

10 **2 Department of Population Health Sciences, School of Public Health, Georgia State**
11 **University, Atlanta, GA, United States of America**

12 **3 Quantori LLC, 625 Mass Ave, Cambridge, MA 02139, United States of America**

13 *** Corresponding author**

14 **E-mail: yuriy.gankin@quantori.com**

15

16

17

18

19 **ABSTRACT**

20 In this work a novel computational multi-reference poly-conformational algorithm is presented for
21 design, optimization, and repositioning of pharmaceutical compounds. The algorithm searches for
22 candidates by comparing similarities between conformers of the same compound and identifies
23 target compounds whose conformers are simultaneously “close” to the conformers for *each* of the
24 compounds in a reference set. The reference compounds can have very different MoAs, which
25 directly and *simultaneously* shapes the properties of the target candidate compounds.

26 The algorithm functionality has been validated *in silico* by scoring ChEMBL drugs against FDA-
27 approved reference compounds which either had the highest predicted binding affinity to our
28 chosen SARS-COV-2 targets or confirmed to be inhibiting such targets in-vivo. All our top scoring
29 ChEMBL compounds also turned out to be either high-affinity ligands to the chosen targets (as
30 confirmed separately in other studies) or showing significant efficacy in-vivo against those
31 selected targets.

32 In addition to method validation *in silico* search for new compounds within two virtual libraries
33 from the Enamine database is presented. The library’s virtual compounds have been compared to
34 the same set of reference drugs that we used for validation: Olaparib, Tadalafil, Ergotamine and
35 Remdesivir. The large reference set of four potential SARS-CoV-2 compounds have been selected,
36 since no drug has been identified to be 100% effective against the virus so far, possibly because
37 each candidate drug was targeting only one particular MoA. The goal here was to introduce
38 methodology for identifying potential candidate(s) that cover multiple MoA-s presented within a
39 set of reference compounds.

40

41

42 **KEYWORDS**

43 conformers, multi-reference, poly-conformational, *in silico*, ligand-based, structure-based, SARS-
44 COV-2, COVID-19, fingerprints, cheminformatics, similarity, virtual library, computational
45 framework, validation.

46

47 **INTRODUCTION**

48 **Conformers as independent molecular entities.** In real life, most compound molecules exist in
49 multiple conformations (shapes) based on the surrounding environmental conditions. In particular,
50 each 3D shape of a molecule dictates its biological activity and enables the molecule to fit into the
51 binding pockets of proteins. Often, distinctly different chemical compounds that have similar
52 shapes (and similar charge distributions along the molecular surface) have a potential to bind as
53 long as the ligand's partial charges are positioned in the binding pocket the same way (i.e., form
54 the same hydrogen bonds). Therefore, it is beneficial to compare the shapes and surface
55 distribution charges for target query and reference compounds on a conformer-by-conformer basis.
56 If one of the conformers of the query molecule matches one of the conformers (especially bound-
57 to-target) of the reference molecule, then there is a chance that the reference compound will also
58 exhibit similar binding properties to the same target.

59 **Alignment-free 3D-similarity scoring.** OpenEye Scientific Software Inc. pioneered an algorithm
60 and the corresponding tool ROCS¹³ for comparing shapes of molecules by overlaying and
61 measuring their molecular structures *in silico* and comparing differences between a query and
62 target molecule. ROCS identifies potentially active compounds by comparing their shapes.

63 Moreover, the ROCS tool is competitive and often superior to structure-based approaches in virtual
64 screening ^{14,15} both in terms of overall performance and consistency ¹⁶. As a result, novel molecular
65 scaffolds have been identified by using ROCS against various targets which have been considered
66 very difficult to address computationally ¹⁷.

67 **Challenges with overlaying.** The process of molecular shapes overlaying remains
68 computationally intensive and often is a bottleneck in the search process for similar molecules.
69 This remains despite the recent so-called PAPER implementation of ROCS on GPU ¹⁸ and the
70 development of FastROCS ¹⁹ for large (>1B) compound libraries. Recently, alternative methods
71 for overlaying have been introduced as a substitute for the ROCS approach. The alternative
72 overlaying is performed by comparing shape-based descriptors (a.k.a conformer-level 3D
73 fingerprints). An example of such an approach is ElectroShape implemented in the ODDT package
74 ²⁰ and is based on the algorithm that incorporates shape, chirality, and electrostatics ^{21,22}, and
75 represents each conformer via a fixed-length vector of real-valued numbers. Similarly the E3FP
76 package ²³ also utilizes an alignment-invariant 3D representation of molecular conformers as a
77 fixed-length binary vector for each conformer. These fingerprint-based approaches allow to
78 calculate the similarity between two molecular shapes either as a Tanimoto distance (for binary
79 fingerprints) or Euclidean distance (for real-valued fingerprints) computations. Such computations
80 are orders of magnitude faster in comparison to alternative methods that require the actual
81 alignment of the two compared conformers. Even though the calculation of a shape-based
82 fingerprint for each conformer can be a rather computationally involved procedure, as soon as all
83 conformers for the virtual library are fingerprinted and stored in a database, the similarity search
84 for the query molecule in such a database is computationally quick. Therefore the computationally

85 efficient method proposed here is expected to be very useful for finding candidate drugs for multi-
86 target disease indications, ligand-based drug design, and drug repurposing applications.

87 **Method applications for SARS-CoV-2 treatment compounds.** The set of SARS-CoV-2
88 treatment compounds have been used for *both* method validation since, there are compounds that
89 have been confirmed to be effective ²⁴ and for the search for new potential compounds based on
90 the existing known set since no drug has been identified to be 100% effective against the virus,
91 possibly because each candidate drug was targeting only one particular MoA²⁵. The SARS-CoV-
92 2 virus has been selected for method illustration because of the importance of the subject. The
93 virus was introduced into the human population in the Chinese city of Wuhan in the Province of
94 Hubei in December of 2019 ¹⁻⁴. Since then the epidemic of SARS-CoV-2 has rapidly spread
95 Worldwide. The World Health Organization (WHO) has officially declared the SARS-CoV-2
96 pandemic in March 2020 just three months after its emergence ⁵. The novel coronavirus received
97 an official name SARS-CoV-2 and the virus pandemic was called COVID-19 ⁶. The formal
98 evaluation and comparison of SARS-CoV-2 drugs can be performed by studying the compound
99 properties by treating patients and performing clinical trials ^{7-10,12} or by studying the properties of
100 the corresponding compounds *in silico* ^{9,11} which is done in this work. For method validation we
101 used public ChEMBL (version 28) database ²⁶ to screen compounds against the most important
102 viral targets, namely 3C-like protease (3CLpro, aka Main protease or Mpro), papain-like protease
103 (PLpro) and RNA-dependent RNA polymerase (RdRp). These targets play a major role in the
104 replication/transcription and host cell recognition and therefore, are vital for the viral reproduction
105 and spread of infection. Because our method doesn't directly use target information but rather
106 analyzes 3D shapes for a compound that was already predicted or experimentally found to be
107 effective against a particular target (we call it a reference compound), one has to choose one (or

108 more) such compound(s) as a reference for each target. The focus for each of the above SARS-
109 COV-2 targets (3CLpro, PLpro and RdRp) was on the reference compounds with the highest
110 binding affinities from the recent in silico multi-target repurposing study.²⁴

111 For the new compound search (virtual library screening) we used the same set of reference
112 compounds as we used for the method validation.

113

114 **METHODS**

115 **Representative conformer space and conformer-by-conformer comparison.** The proposed
116 computational algorithm extends the currently available methods²⁰⁻²³ and introduces additional
117 search flexibility via the use of the compound conformers. The proposal is to compare multiple
118 possible shapes, adopted via varying environmental conditions, of the same molecule (i.e.,
119 conformers) rather than just a single shape that was used before. In particular, the suggested
120 approach is based on the matching of ligand-ligand fingerprints without explicitly using target
121 structure information unlike docking and molecular dynamics approaches that simulate physical
122 binding of a ligand to the target. The supporting theory behind the method is based on the decision
123 to treat conformers, which might have different binding characteristics and properties, as
124 independent entities. In such an approach each conformer has the corresponding independent
125 alignment-free 3D-similarity scoring using the known multi-references. All conformers were
126 generated using the ETKDG algorithm implemented in RDkit²⁷. Benchmarking studies have
127 found ETKDG to be the best-performing freely available conformer generator up-to-date^{28,29}
128 providing diverse and chemically-meaningful conformers reproducing crystal conformations.

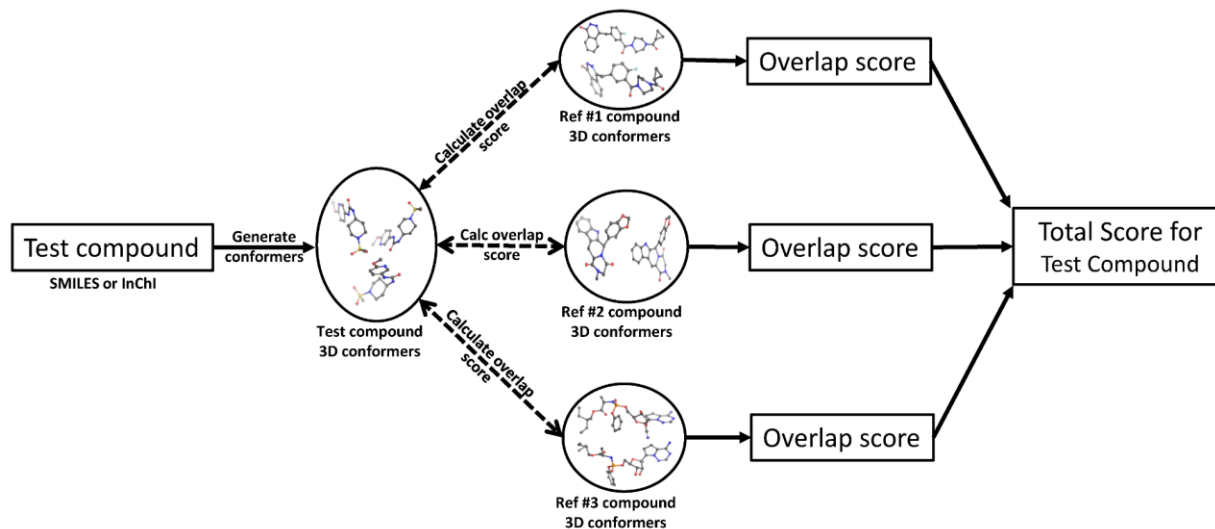
129 Unlike what the majority of computational methods had assumed a couple of decades or so ago
130 (e.g. in the CoMFA method ⁵⁸), recent research indicates that the bioactive conformation is not
131 necessarily the lowest-energy conformation in the presence of the receptor ⁵⁹⁻⁶¹. In particular, as
132 long as an increase in energy for less favorable conformation is compensated by its binding to the
133 target, i.e. the total ligand-target energy is lower than the sum of the energies for the non-bound
134 target and ligand, the bound state is favored. The proposed method emphasizes and relies on this
135 ligand's ability to use its potentially higher energy conformations depending on the target it
136 attempts to bind. Note, however, that when a sufficiently large number of conformers is requested,
137 ETKDG algorithm generates more conformers with lower energy than with higher energy ^{27,28},
138 therefore when averaged over all conformers (and we generate 100 conformers per molecule),
139 conformers with the lower energy will contribute more to the total overlap.

140 Actually, one of the things that distinguishes ligand-based 3D virtual screening methods from 2D
141 methods is that one has to start worrying about how many conformers to include in the reference
142 set. If the molecule is flexible, it can assume many shapes and pharmacophores. How to deal with
143 this is one of the fundamental questions in ligand-based virtual screening (LBVS).

144 In a recent paper by Schrödinger team ³⁰ Cappel *et al.* performed comprehensive benchmark
145 analysis and found that the number of conformers needed for 3D LBVS is actually relatively low:
146 100 or less to achieve good performance. Thus, we used ETKDG to generate 100 conformers per
147 molecule in this work.

148 The authors have called the approach MultiRef3D to emphasize that it is a fast, alignment-free
149 multi-objective optimization protocol that maximizes the 3D overlap of a query molecule's
150 conformational ensemble with conformational ensembles of multiple reference ligands. The

151 diagram of the proposed method is summarized in Fig. 1. The formal details of the approach are
152 discussed further.



153
154 **Fig. 1.** MultiRef3D screening method diagram for multi-conformer and multi-reference screening
155 procedure. For each test compound multiple conformers and the corresponding overlapping scores
156 are computed. Later, the overlapping scores are summed into the total score for the selected test
157 compound. Figure has been created in Microsoft PowerPoint 2016, pyMOL v2.5 (pymol.org) and
158 RDKit v2021.03.01 software (rdkit.org).

159
160 **Efficiency and a conformer scoring.** In the algorithm, each conformation is treated as an
161 independent entity and is characterized by a vector of features (fingerprint) which describes its 3D
162 shape along with the distribution of electrostatic charge (both denoted further as electroshape)
163 across its molecular surface. In this work we used 15-dimensional USRCAT fingerprints³¹ which
164 distil molecular shape into a rotation-invariant descriptor vector made up of 15 real numbers
165 describing distance distribution among atoms, atomic partial charges and atom types. USRCAT

166 fingerprints were shown to significantly outperform just shape-based fingerprints in recent
167 benchmark tests^{31,32}. Since USRCAT fingerprints reflect both relative 3D positions for all atom
168 types and molecular surface charges for each query molecule conformer as well as for all
169 conformers of the reference compound they are very well-suited for alignment-free fast
170 computation of conformer similarity. Each conformer is coded within the algorithm by a single
171 fingerprint represented as a fixed-length vector of numbers which ensures computational
172 efficiency. These fingerprints for each of the query and reference molecule conformers are
173 individually scored by Euclidean distance serving as a similarity measure between two conformers.
174 The Euclidean distance can be viewed as an extension of the Tanimoto similarity measure for non-
175 binary fingerprints. The fingerprinting of individual conformers for alignment-free comparisons
176 became popular in the past couple of years^{23,33-35} so the proposed method is built on those.

177 **Objective Function Optimization.** The sum of the conformer-to-conformer similarity scores
178 between the query and a reference compound are compared via an objective similarity function W_c
179 for each reference compound c . The goal is to maximize the sum of those individual objective
180 similarity functions across all reference compounds of interest $c=1,2,\dots,C$ where c is a summation
181 index for the desired set of reference compounds:

$$182 \quad W_{All} = \sum_{c=1}^C W_c = \sum_{c=1}^C \sum_{q=1}^Q \sum_{r=1}^R S_{q,r}^{(c)} \quad (1)$$

183 In formula (1) the summand $S_{q,r}^{(c)}$ is the similarity (overlap) of the query conformer q ($q=1,2,\dots,Q$)
184 with the conformer r ($r=1,2,\dots,R$) for each reference compound c ($c=1,2,\dots,C$). For the real-valued
185 fingerprints, the similarity summand between the pair of conformers of interest indexed by query
186 index q and reference index r for compound c is calculated as:

187
$$S_{q,r}^{(c)} = 1 - (1/N) \sqrt{\sum_{n=1}^N (x_{q,n}^{(c)} - x_{r,n}^{(c)})^2} \quad (2)$$

188 where $x_{q,n}^{(c)}$ and $x_{r,n}^{(c)}$ are the corresponding normalized fingerprint vector coordinates for
189 $n=1,2,\dots,N$. The length (the number of coordinates) of the fingerprint N is determined based on
190 the problem-specific target-ligand interaction characteristics. Since the fingerprint coordinates $x_{q,n}^{(c)}$
191 and $x_{r,n}^{(c)}$ are normalized (i.e. have values between 0 and 1 for each coordinate n) the resulting
192 overlap $S_{q,r}^{(c)}$ is maximized with the value equal to 1 when the fingerprints of both conformers are
193 identical and can take the smallest value equal to 0 when all the fingerprint coordinates have a
194 difference equal to 1 i.e. as different as possible at the normalized scale.

195 When the objective is to identify a novel compound for just a single active conformation ($r=1$) of
196 one ($c=1$) reference compound (e.g. a reference ligand co-crystallized with one particular target)
197 then all conformers for the query molecule are scored against only one active reference conformer.
198 However, in the case when multiple reference compounds are bound to the same target (or sets of
199 reference compounds bound to multiple targets), the total objective function comes into play. It is
200 important to point out that the proposed method is not limited to the structure-based design
201 situations: when several reference compounds are found to be active in a functional assay (and
202 either the target(s) is unknown or the crystal structure of the target is not available) - the formula
203 works just as well (as long as the ligand structure is known). The method becomes especially
204 handy, when there is a great diversity among active reference compounds, whether the target
205 structural information is known or not – the objective function will extract and sum up the
206 similarities for all of the relevant parts of the fingerprinted conformer representations responsible
207 for the observed activity.

208 The query compound can be evaluated against multiple reference compounds on a conformer-by-
209 conformer basis. In such a case, the corresponding similarity scores are summed and constitute
210 the multi-reference conformer-level objective function to maximize. This can be readily used in a
211 typical ligand-based design setting. However, instead of just searching for a shape analog of one
212 of the conformers of a reference compound, in the case of multiple references, the algorithm
213 performs a search for such a compound in the virtual library whose conformers have overlapped
214 with conformers of each of those reference compounds. The latter will increase the chances that
215 the selected virtual compound binds the same way to the corresponding targets of each of the
216 references (i.e. the selected compound is capable of forming conformations that resemble active
217 conformations responsible for the MoA of each of the references).

218 **Method validation for known targets.** To validate the proposed methodology for the multi-
219 target-specific conformer similarity the three following targets have been used: 3CLpro (Mpro),
220 PLpro, and RdRp. The spike protein has not been included as the validation target since the
221 pharmacological activity may not be correlated directly with the binding affinity to the interfacial
222 site²⁴. ChEMBL (version 28) public database²⁶ has been chosen as the universe for screening. The
223 selected ChEMBL compounds were already marketed drugs for which at least one target is known.
224 The corresponding ChEMBL extraction query is provided in the manuscript Supplement at GitHub
225 (<https://github.com/quantori/MultiRef3D>). The screened set had a total of 2,604 compounds. The
226 corresponding reference compounds for validation were selected from the recent multi-target *in*
227 *silico* repurposing study²⁴ based on the highest binding affinities for each of the SARS-COV-2
228 three targets 3CLpro, PLpro and RdRp.

229 **Compounds search based on reference compounds' conformers.** One hundred conformers for
230 each of the reference molecules were generated at the MMFF94 level of theory⁴⁰ and each

231 conformer was ODDT-fingerprinted ²⁰ and saved in the MongoDB database ⁴¹. The ODDT
232 implementation ²⁰ of ElectroShape fingerprints ²² has been selected to demonstrate the proposed
233 approach because these fingerprints are considered to be state-of-the-art in ligand-based virtual
234 screening experiments ^{32,42}, and they are not limited to binary values.

235 **Virtual libraries for screening.** Virtual libraries (query compounds) for screening consisted of
236 Enamine⁴¹ focused “antiviral-like” set (3,995 compounds) and diverse Discovery Diversity Set
237 (10,559 compounds) ⁴⁴. Molecules from each virtual library were simultaneously evaluated against
238 several reference drugs with different MoA (3CLpro, PLpro and RdRp inhibition). A query
239 molecule for which some of its conformers are similar in shape with conformers for all the
240 reference drugs would receive a higher score. In this approach, multiple virtual compounds can be
241 identified to have a good conformer overlap with conformers of the reference drugs.

242

243 **RESULTS**

244 **Method Validation for SARS-CoV-2 Compounds.** The highest affinity binder Olaparib (-9.2
245 kcal/mol) has been selected as a reference compound for 3CLpro, Tadalafil (-9.2 kcal/mol) for
246 PLpro and Lumacaftor (-9.9 kcal/mol) for RdRp. However, when multi-target scoring against
247 these three references has been performed, the top ten scoring compounds from ChEMBL *had no*
248 *conformers* similar in 3D shape (Euclidean distance < 0.5) to Lumacaftor conformers. Therefore,
249 the Lumacaftor reference has been replaced with the next best *in silico* RdRp
250 binder²⁴Ergotamine²⁴ (-9.4 kcal/mol binding affinity to RdRp). The resulted scores produced by
251 the proposed method are summarized in Tab. 1:

252

253

254

255 **Tab. 1.** Top ten scoring compounds showing simultaneous conformer similarity with the reference
 256 compounds Olaparib, Tadalafil, and Ergotamine.

Compound ID	Compound Name	TotalScore	Olaparib	Tadalafil	Ergotamine
CHEMBL779	Tadalafil	228.46	70.70	100.00	57.76
CHEMBL1737	Sildenafil citrate	225.15	81.30	58.34	85.50
CHEMBL521686	Olaparib	223.08	100.00	57.61	65.48
CHEMBL105442	Ci-1040	220.40	80.68	79.16	60.56
CHEMBL129857	As-602868	220.16	78.27	74.50	67.39
CHEMBL2037511	Epelsiban	219.86	81.58	70.28	68.01
CHEMBL565612	Sotrastaurin	219.13	79.93	69.36	69.83
CHEMBL1516474	Tegaserod maleate	217.83	80.22	76.56	61.05
CHEMBL1236682	Refametinib	217.78	76.01	81.57	60.20
CHEMBL1923502	Ulimorelin hydrochloride	217.56	76.29	74.79	66.47

257

258 Both Olaparib and Tadalafil had the highest scores which confirmed the previous finding²⁴ that
 259 these compounds are simultaneously good binders for *both* 3CLpro and PLpro. Our method has
 260 also picked up Sildenafil (more commonly known under the brand name Viagra) which just like
 261 Tadalafil (aka Cialis) is also known as a classical PDE5A inhibitor. Although those compounds
 262 are predominantly used in the treatment of male erectile dysfunction and pulmonary hypertension,

263 it was shown ⁴⁵ that in the presence of SARS-COV-2 infection, PDE5 inhibitors prevent
264 thromboembolism caused by inflammatory processes in COVID-19 patients via NO/cGMP
265 pathway and are potent inhibitors of 3CLpro ⁴⁶

266 Ci-1040 and Refametinib are the other two hits from Tab. 1 and are potent MEK inhibitors with
267 high 3D shape similarity to both Olaparib and Tadalafil. MEK inhibitors, including Olaparib⁴⁷
268 were recently demonstrated to reduce cellular expression of ACE2 while stimulating NK-mediated
269 cytotoxicity and attenuating inflammatory cytokines during the severe stage of SARS-CoV-2
270 infection⁴⁸. Ci-1040 was also previously shown to display a broad anti-influenza virus activity in
271 vitro and to provide a prolonged treatment window compared to the standard of care in vivo,
272 specifically in lung cells⁴⁹.

273 The other hit from Tab. 1 is Sotrastaurin which is a PKC inhibitor and has been experimentally
274 shown to inhibit SARS-COV-2 replication in vivo ⁵⁰and has been found to be among the best
275 3CLpro binders during *in silico* ZINC database screening study ⁵¹ Yet another notable hit among
276 the top ten selected compounds in Tab. 1 is As-602868: a potent IKK2 inhibitor. This class of
277 compounds is currently preclinically tested for NF-kB mediated cytokine storm attenuation in
278 severe COVID-19 patients ⁵².

279 The other top hit, Epelsiban, was originally developed as an oxytocin receptor agonist. However,
280 it has been recently shown ⁵⁴ that oxytocin plays a major role in activation of NF-kB-mediated
281 pathways. Interestingly, recent research has revealed ⁵⁰ that Remdesivir (in addition to being a
282 potent RdRp inhibitor) is also reducing viral replication via NF-kB pathway. Therefore, this hit
283 serves as an example of non-obvious 3D-shape-based drug repurposing idea generation linked to
284 the relevant yet non-primary SARS-COV-2 inhibiting mechanisms of reference compounds.

285 Thus in our second validation experiment the RdRp reference compound Ergotamine has been
286 replaced with Remdesivir which, as we already mentioned, is a well-established RdRp inhibitor
287 and cytokine storm attenuator that works via NF- κ B pathway. The resulted scores produced in the
288 second scoring setup are summarized in Tab. 2:

289 **Tab. 2.** Top ten scoring compounds showing simultaneous conformer similarity with the reference
290 compounds Olaparib, Tadalafil, and Remdesivir.

Compound ID	Compound Name	TotalScore	Olaparib	Tadalafil	Remdesivir
CHEMBL1694	Benazepril hydrochloride	180.82	66.67	64.26	49.89
CHEMBL515606	Cilazapril	180.61	64.56	61.56	54.50
CHEMBL495727	At-9283	179.03	68.17	56.15	54.71
CHEMBL2107495	Temafloxacin hydrochloride	178.94	67.15	55.78	56.01
CHEMBL1200779	Trovafloxacin mesylate	178.60	66.24	54.02	58.35
CHEMBL340978	Benoxaprofen	178.27	68.56	56.54	53.16
CHEMBL8	Ciprofloxacin	177.05	63.21	57.19	56.65
CHEMBL1200831	Spirapril hydrochloride	177.00	65.28	60.24	51.47
CHEMBL1201011	Quinapril hydrochloride	176.84	66.32	60.40	50.13
CHEMBL1168	Ramipril	176.54	65.32	63.26	47.96

291

292 For Olaparib, Tadalafil, and Remdesivir reference compounds half of the top ten hits
293 (Benoxaprofen, Ciprofloxacin, Spirapril hydrochloride, Quinapril hydrochloride and Ramipril)
294 turned out to be ACE inhibitors and coagulation modifiers acting via NF-kB related pathways^{55,56}!
295 In addition, all of them turned out to be also good binders of 3CLpro⁵⁷.

296 The other hits were Temafloxacin and Trovafloxacin, predicted to be potent 3CLpro ligands⁵⁵ and
297 experimentally shown to inhibit virus replication^{56,57}, and anti-inflammatory drugs Benoxaprofen
298 and Ciproflaxin predicted to target 3CLpro^{58,59} as well.

299 Concluding the list is an interesting multi-target Aurora/JAK inhibitor hit: compound At-9283.
300 JAK inhibitors, in general, have promising therapeutic potential for SARS-COV-2 treatment with
301 their dual anti-inflammatory and anti-viral effects⁶⁰. At-9283, however, has also been recently
302 identified to reverse SARS-COV-2 transcriptomic signature⁶¹ and due to its matching tipiracil's
303 3D pharmacophore scaffold also inhibits SARS-COV-2 Nsp15 endoribonuclease^{62,63} and targets
304 3CLpro as well^{64,65}.

305 **Virtual library screening for multi-target SARS-CoV-2 compounds.** The results from the
306 focused (“antiviral-like”) and diverse (“Discovery Diversity Set”) are summarized in Tab 1 and 2
307 respectively. . The algorithm visual summary is displayed in Fig. 1 for the W_{All} objective function.
308 Tables 3 and 4 summarize the direct application results of the Enamine⁴¹ focused “antiviral-like”
309 and “Diverse Discovery Set” virtual library screening. The first two columns of the Tables contain
310 query compound IDs and their computed overlap scores. The rows are sorted according to the total
311 sum overlap score displayed in the second column.

312

313 **Tab. 3.** The top scoring compounds from the Enamine “antiviral-like” virtual library (the first
314 column) are sorted by their total overlap score W_{All} (the second column). The values in the other
315 columns correspond to the sums of the overlap scores of the conformers for the corresponding
316 reference compounds.

Compound ID	Wall	Olaparib	Tadalafil	Ergotamine	Remdesivir
Z1693453146	254.11	71.68	56.30	76.76	49.38
Z434669842	248.84	66.18	55.33	69.92	57.41
Z1381427631	248.57	66.63	52.86	72.84	56.24
Z1381425049	247.97	66.09	53.03	71.98	56.88
Z1313285936	246.97	67.70	55.51	72.23	51.54
Z826278840	246.37	65.61	56.67	68.79	55.30
Z94559538	245.69	70.41	55.41	65.24	54.64
Z435640438	245.21	63.85	54.62	72.45	54.29
Z435642248	245.13	64.04	55.31	71.85	53.93
Z827564114	244.89	64.93	57.02	70.19	52.75

317

318

319

320

321

322 **Tab. 4.** The top scoring query compounds from the Enamine a “Diverse Discovery Set” virtual
323 library (the first column) are sorted by their total overlap score W_{All} (the second column). The
324 values in the other columns correspond to the sums of the overlap scores of the conformers for the
325 corresponding reference compounds.

Compound ID	Wall	Olaparib	Tadalafil	Ergotamine	Remdesivir
Z1760146546	255.19	74.41	60.57	74.94	45.27
Z3077896041	254.26	67.67	57.38	75.53	53.67
Z2911083836	253.23	72.49	58.63	75.85	46.27
Z2446617864	252.49	73.18	59.52	75.06	44.72
Z1139281415	252.30	69.01	57.39	75.88	50.02
Z1354703942	251.79	77.22	61.63	80.63	32.32
Z2256366543	251.27	66.54	54.27	74.18	56.28
Z1139281396	250.99	68.40	57.90	74.43	50.27
Z1139280685	250.51	68.34	57.88	74.50	49.79
Z2959367287	250.32	69.54	55.40	72.80	52.58

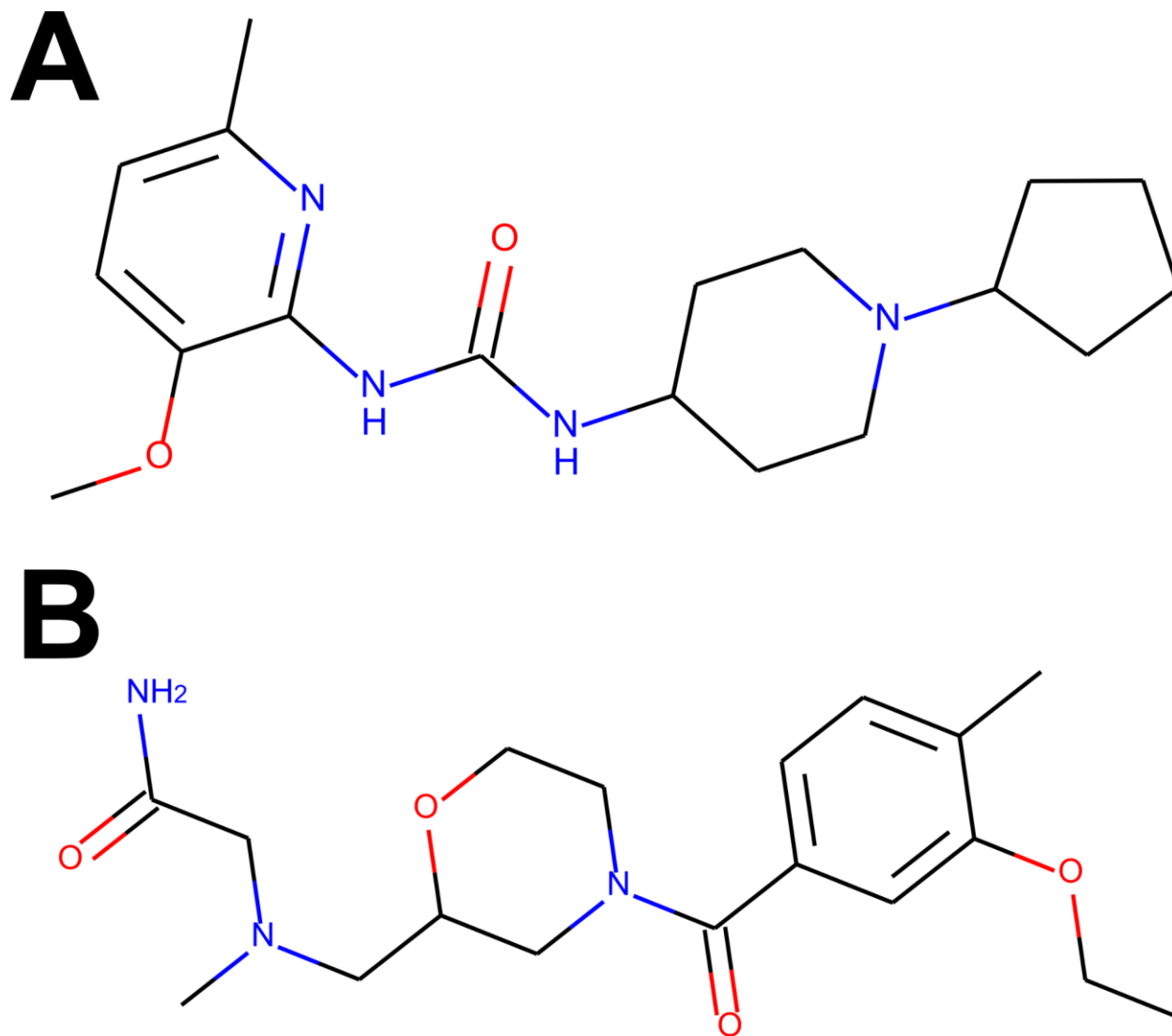
326
327 For the visual illustration of the algorithm results two compounds with the highest scores from
328 Tab. 3 and 4 have been presented in Fig. 2, panels A and B respectively. It is worth noting that
329 these compounds are quite flexible molecules due to their amidebridge around which the ring
330 substructures can rotate, which ensures the ability of those molecules to accommodate different
331 targets.

332

333

334

335



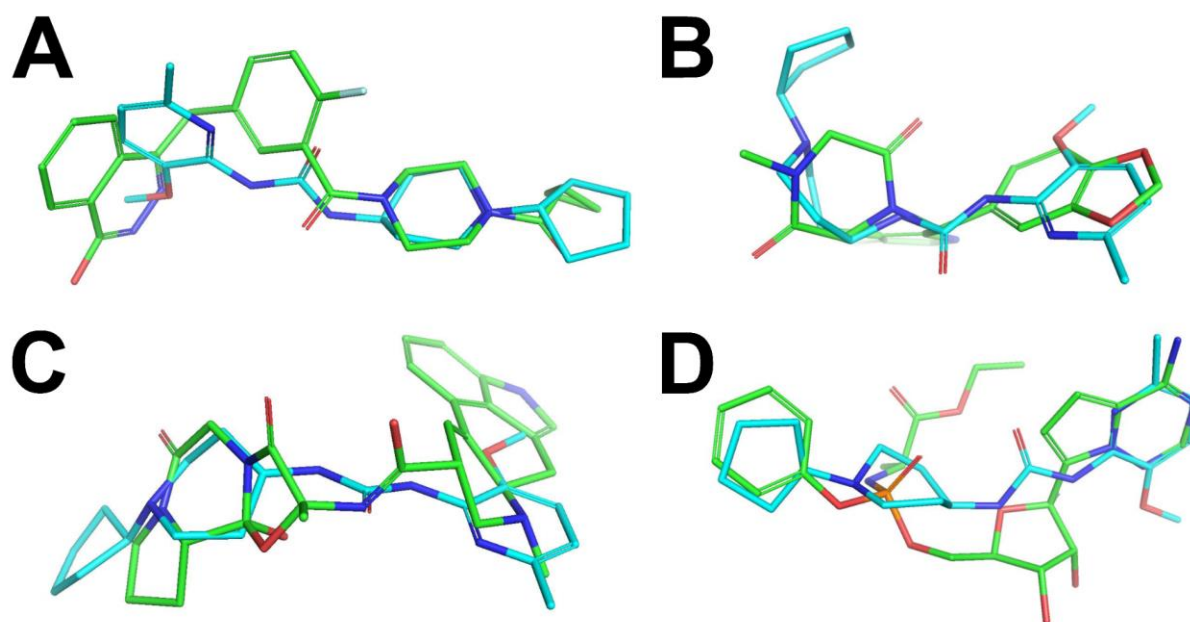
336

337 **Fig. 2.** The compounds presented in panels A and B are the top hits Z1693453146 (*Wall* = 254.11)
338 and ZZ1760146546 (*Wall* = 255.19) from the non-overlapping “antiviral-like” and “Discovery
339 Diversity” libraries respectively. One can immediately observe, however, that the compounds
340 share a lot of similarity, in particular overall shape and amide bridge connecting heterocycles. The

341 bridge allows for 3D flexibility for the molecule to change conformation and bind to multiple
342 targets. Figure has been created in Microsoft PowerPoint 2016, pyMOL v2.5 (pymol.org) and
343 RDKit v2021.03.01 software (rdkit.org).

344 Fig. 3 demonstrates how the best-matching conformers of the top hit Z1693453146 spatially align
345 with the active conformation for each reference drug. One can observe that the majority of
346 hydrogen donors and acceptors from the top hit conformer and reference conformers are aligned
347 very well mimicking the interaction patterns with each target. At least partial spatial alignment of
348 atom types is expected from the top hit conformers since atom types as well as their relative 3D
349 positions is the essence of the USRCAT fingerprints³¹.

350



351

352 **Fig. 3.** Active conformers of the Reference compounds (Olaparib, Tadalafil, Ergotamine and
353 Remdesivir on panels A, B, C and D respectively) aligned with the best matching conformers of
354 the top hit Z1693453146 (Wall = 254.11). Carbon-carbon bonds for the reference compounds and

355 the tTop hHit are shown in green and cyan respectively (C-N and C-O bonds are conventionally
356 shown in blue and red). Figure has been created in Microsoft PowerPoint 2016, pyMOL v2.5
357 (pymol.org) and RDKit v2021.03.01 software (rdkit.org).

358

359 **DISCUSSION**

360 **Computation efficiency and availability of the method.** The proposed method does not rely on
361 laborious docking and molecular dynamics setup, especially in the multi-target case, where target
362 preparation and choice of method i.e. direct docking to a fixed-coordinate target or Molecular
363 Dynamics -based ensemble energy minimization are of utmost importance and require deep
364 expertise. Fingerprint comparison is orders of magnitude faster and simpler (only requires simple
365 structural information in the form of either isomeric SMILES or InChI). The entire setup is
366 presented in our Supplement that can be universally used for any multi-target screening and
367 optimization whenever reference compounds for each of the targets are available. Naturally,
368 further hit refinement (ADMETox, PK/PD, etc) is necessary if the screened universe is not limited
369 to the drugs with the well-known safety profiles.

370 **Application for drug-repurposing.** Depending on what is known about the indication or
371 marketed drug of interest (targets, MoAs, other existing drugs for the same indication) the
372 proposed methods (or a combination thereof) can be used to find other non-obvious molecules
373 whose shape and the surface electrostatic charge is similar to that of the marketed drug. The
374 methods can also be used to search for the cumulative similarity to conformers of the multiple
375 drugs used to treat this disease indication.

376 In the proposed approach multiple conformers of the query ligand have been compared with
377 conformers from *multiple* reference compounds whose therapeutic effect of interest is achieved
378 via different mechanisms of bindings to different targets, e.g. by inhibiting major proteases
379 3CLpro and PLpro⁶³ and RNA-dependent RNA polymerase (RdRp)^{64,65,66}. An “ideal drug” would
380 contain conformers that resemble (as many as possible) conformers of all of the reference drugs,
381 thus increasing chances that the drug inhibits SARS-CoV-2 via multi-MoA routes and is more
382 effective than each individual reference drug.

383 **Note on applications for structure-based designs.** When the crystal structure of the target protein
384 is known and the reference ligand is co-crystallized in its active conformation (structure-based
385 design), we can use this information about the reference compound and evaluate the query
386 molecules against only one, the active (co-crystallized) reference ligand conformation ($r = r_{active}$)
387 in formulas (1) and (2). Confirmation by direct docking for the fingerprint-matched queries can be
388 used to confirm the match.

389 Our methodology emphasizes pursuit of candidate compounds that achieve therapeutic effect (e.g.
390 stops SARS-CoV-2 proliferation) by multiple MoA routes. A successful candidate compound
391 would contain conformers targeting the two major proteases 3CLpro and PLpro RdRpall at the
392 same time by increasing chances that the compound would protect against SARS-CoV-2 much
393 more effectively. Naturally, all successful candidates would need to be further screened and
394 filtered for proper ADME-Tox and other drug-likeness properties. Binding to anti-targets, e.g.
395 hERG, can be explicitly incorporated to this methodology by adding the corresponding terms
396 (similarities to known hERG-binding ligands) to the overlap sum with a negative sign. Even
397 though many computational methods exist to evaluate hERG in particular as well as other common
398 tox liabilities, when an anti-target is very specific and less commonly known as “pure tox target”

399 (e.g. undesired binding to D2 receptor for many modern CNS drugs), the explicit inclusion of
400 similarity score to such anti-target with a negative sign can greatly streamline the overall drug
401 optimization process.

402

403 **CONCLUSION**

404 We have demonstrated and validated the usefulness of the multi-reference computationally
405 efficient optimization approach in drug discovery screening and repurposing scenarios. The
406 method represents each molecule as an ensemble of flexible conformers that would choose the
407 best possible conformation for each presented target-binding opportunity. Application of this
408 approach to SARS-CoV-2 produced several antiviral drug candidates that are designed to protect
409 against SARS-CoV-2 by multiple mechanisms simultaneously.

410

411 **LIST OF ABBREVIATIONS**

412 ADME-Tox - Absorption, Distribution, Metabolism, Excretion and Toxicity

413 GPU - Graphics processing unit

414 CNS - Central nervous system

415 CoMFA - Comparative molecular field analysis

416 COVID-19 - Coronavirus Disease of 2019

417 CPU - Central processing unit

418 hERG - Human Ether-a-go-go-related Gene

419 MoA(s) - Mechanism of Action(s)

420 ODDT - Open Drug Discovery Toolkit

421 RNA - Ribonucleic acid

422 ROCS - Rapid overlay of chemical structures

423 SARS-CoV-2 - Severe acute respiratory syndrome coronavirus 2

424 WHO - World Health Organization

425

426 **DECLARATIONS**

427 **Availability of data and materials**

428 Code that has been used for analysis and for manuscript preparation can be found at Quantori
429 public GitHub repository online ⁶⁷. Data (ligand structures) from REAL focused libraries can be
430 downloaded from the Enamine Ltd. website ⁶⁸.

431 **Competing interests**

432 The proposed method has been submitted for a patent. The patent application number is 63061790
433 at the United States Patent and Trademark Office and as of October 17, 2020, the patent is pending.
434 The patent can be a source of financial income for authors Vadim Alexandrov (VA) and Yuriy
435 Gankin (YG).

436

437

438 **Funding**

439 The author Vadim Alexandrov (VA), a founder of a consulting company Liquid Algo LLC in
440 Hopewell Junction, New York, United States received no compensation for this work. The author
441 Yuriy Gankin (YG) is employed by the commercial company Quantori in Cambridge,
442 Massachusetts, United States. Alexander Kirpich (AK) is employed at the School of Public Health
443 at a non-profit institution Georgia State University. Quantori provided support in the form of salary
444 and relevant publication and patent fees for YG. YG received no compensation for this work. AK
445 received no funding or any other financial support for this project.

446 **Authors' contributions**

447 Vadim Alexandrov (VA), Alexander Kirpich (AK), and Yuriy Gankin (YG) are the authors of the
448 manuscript. VA and YG proposed the manuscript idea, obtained the data, implemented routine
449 coding operations, and wrote the preliminary version of the manuscript. AK performed an
450 additional literature review and wrote the final version of the manuscript. YG also provided the
451 overall guidance for the project and participated in the manuscript preparation.

452 **Acknowledgments**

453 The authors would like to acknowledge Nika Tsutskiridze and Daviti Khatchilava for their
454 assistance in extracting information from clinical trials and peer reviewed literature. The authors
455 also want to acknowledge Alexander Proutsky and John Reynders for their suggestions and
456 comments during the manuscript preparation.

457 **Authors' information**

458 VA holds a Ph.D. in Computational Chemistry from The University of Arizona and a Ph.D. in
459 BioInformatics from Yale University. He has over 20 years of experience in computer-aided drug
460 design and pioneered hit generation and lead optimization paradigm in high-throughput in-vivo
461 phenotypic drug discovery.

462 AK is a biostatistician and an assistant professor in the Department of Population Health Sciences
463 at the School of Public Health at Georgia State University. AK holds a Ph.D. in biostatistics from
464 the University of Florida and has expertise in infectious disease statistical modeling (cholera,
465 dengue, HIV, anthrax, and others), epidemiology, and bioinformatics. The interests and goals of
466 AK are broad and target application of statistical methods to public health and biomedical research
467 questions and policies and to address statistical challenges, such as missing data, asymptomatic
468 infections, underreporting, and noise during data acquisition.

469 YG serves as Chief Scientific Officer at Quantori, a developer of intelligent IT and data science
470 solutions for life science, pharma, and healthcare organizations. Yuriy's expertise is in analytical
471 chemistry, data science, and chem- and bioinformatics. He holds a Ph.D. in Analytical Chemistry
472 from Tufts University and an MBA from the Massachusetts Institute of Technology Sloan School
473 of Management.

474

475

476

477

478

479

480 **REFERENCES**

- 481 1. Zhu, N. *et al.* A Novel Coronavirus from Patients with Pneumonia in China, 2019. *N. Engl.*
482 *J. Med.* **382**, 727–733 (2020).
- 483 2. Lu, H., Stratton, C. W. & Tang, Y.-W. Outbreak of pneumonia of unknown etiology in
484 Wuhan, China: The mystery and the miracle. *J. Med. Virol.* **92**, 401–402 (2020).
- 485 3. Huang, C. *et al.* Clinical features of patients infected with 2019 novel coronavirus in
486 Wuhan, China. *The Lancet* vol. 395 497–506 (2020).
- 487 4. Chen, N. *et al.* Epidemiological and clinical characteristics of 99 cases of 2019 novel
488 coronavirus pneumonia in Wuhan, China: a descriptive study. *The Lancet* vol. 395 507–513
489 (2020).
- 490 5. WHO Director-General’s opening remarks at the media briefing on COVID-19 - 11 March
491 2020. [https://www.who.int/dg/speeches/detail/who-director-general-s-opening-remarks-at-](https://www.who.int/dg/speeches/detail/who-director-general-s-opening-remarks-at-the-media-briefing-on-COVID-19---11-march-2020)
492 [the-media-briefing-on-COVID-19---11-march-2020.](https://www.who.int/dg/speeches/detail/who-director-general-s-opening-remarks-at-the-media-briefing-on-COVID-19---11-march-2020)
- 493 6. Naming the coronavirus disease (COVID-19) and the virus that causes it.
494 [https://www.who.int/emergencies/diseases/novel-coronavirus-2019/technical-](https://www.who.int/emergencies/diseases/novel-coronavirus-2019/technical-guidance/naming-the-coronavirus-disease-(covid-2019)-and-the-virus-that-causes-it)
495 [guidance/naming-the-coronavirus-disease-\(covid-2019\)-and-the-virus-that-causes-it.](https://www.who.int/emergencies/diseases/novel-coronavirus-2019/technical-guidance/naming-the-coronavirus-disease-(covid-2019)-and-the-virus-that-causes-it)
- 496 7. Cascella, M., Rajnik, M., Cuomo, A., Dulebohn, S. C. & Di Napoli, R. Features,
497 Evaluation, and Treatment of Coronavirus (COVID-19). in *StatPearls [Internet]* (StatPearls
498 Publishing, 2020).
- 499 8. Sanders, J. M., Monogue, M. L., Jodlowski, T. Z. & Cutrell, J. B. Pharmacologic
500 Treatments for Coronavirus Disease 2019 (COVID-19): A Review. *JAMA* (2020)
501 doi:10.1001/jama.2020.6019.
- 502 9. Elmezayen, A. D., Al-Obaidi, A., Şahin, A. T. & Yelekçi, K. Drug repurposing for

- 503 coronavirus (COVID-19): screening of known drugs against coronavirus 3CL hydrolase and
504 protease enzymes. *J. Biomol. Struct. Dyn.* 1–13 (2020).
- 505 10. Zhang, W. *et al.* The use of anti-inflammatory drugs in the treatment of people with severe
506 coronavirus disease 2019 (COVID-19): The experience of clinical immunologists from
507 China. *Clin. Immunol.* 108393 (2020).
- 508 11. Beck, B. R., Shin, B., Choi, Y., Park, S. & Kang, K. Predicting commercially available
509 antiviral drugs that may act on the novel coronavirus (SARS-CoV-2) through a drug-target
510 interaction deep learning model. *Comput. Struct. Biotechnol. J.* **18**, 784–790 (2020).
- 511 12. Sargiacomo, C., Sotgia, F. & Lisanti, M. P. COVID-19 and chronological aging: senolytics
512 and other anti-aging drugs for the treatment or prevention of corona virus infection? *Aging*
513 **12**, 6511–6517 (2020).
- 514 13. Rocs, O. E. OpenEye Scientific Software, Inc., Santa Fe, NM, USA. (2008).
- 515 14. Hawkins, P. C. D., Skillman, A. G. & Nicholls, A. Comparison of shape-matching and
516 docking as virtual screening tools. *J. Med. Chem.* **50**, 74–82 (2007).
- 517 15. Venhorst, J., Núñez, S., Terpstra, J. W. & Kruse, C. G. Assessment of scaffold hopping
518 efficiency by use of molecular interaction fingerprints. *J. Med. Chem.* **51**, 3222–3229
519 (2008).
- 520 16. Sheridan, R. P., McGaughey, G. B. & Cornell, W. D. Multiple protein structures and
521 multiple ligands: effects on the apparent goodness of virtual screening results. *J. Comput.*
522 *Aided Mol. Des.* **22**, 257–265 (2008).
- 523 17. Rush, T. S., 3rd, Grant, J. A., Mosyak, L. & Nicholls, A. A shape-based 3-D scaffold
524 hopping method and its application to a bacterial protein-protein interaction. *J. Med. Chem.*
525 **48**, 1489–1495 (2005).

- 526 18. Haque, I. S. & Pande, V. S. PAPER--accelerating parallel evaluations of ROCS. *J. Comput.*
527 *Chem.* **31**, 117–132 (2010).
- 528 19. FastROCS. OpenEye Scientific Software, Inc., Santa Fe, NM, USA. (2011).
- 529 20. Wójcikowski, M., Kukielka, M., Stepniewska-Dziubinska, M. M. & Siedlecki, P.
530 Development of a protein-ligand extended connectivity (PLEC) fingerprint and its
531 application for binding affinity predictions. *Bioinformatics* **35**, 1334–1341 (2019).
- 532 21. Ballester, P. J. & Richards, W. G. Ultrafast shape recognition to search compound databases
533 for similar molecular shapes. *J. Comput. Chem.* **28**, 1711–1723 (2007).
- 534 22. Armstrong, M. S. *et al.* ElectroShape: fast molecular similarity calculations incorporating
535 shape, chirality and electrostatics. *J. Comput. Aided Mol. Des.* **24**, 789–801 (2010).
- 536 23. Axen, S. D. *et al.* A Simple Representation of Three-Dimensional Molecular Structure. *J.*
537 *Med. Chem.* **60**, 7393–7409 (2017).
- 538 24. Murugan, N. A., Kumar, S., Jeyakanthan, J. & Srivastava, V. Searching for target-specific
539 and multi-targeting organics for Covid-19 in the Drugbank database with a double scoring
540 approach. *Sci. Rep.* **10**, 1–16 (2020).
- 541 25. Recent progress and challenges in drug development against COVID-19 coronavirus
542 (SARS-CoV-2) - an update on the status. *Infect. Genet. Evol.* **83**, 104327 (2020).
- 543 26. Gaulton, A. *et al.* ChEMBL: a large-scale bioactivity database for drug discovery. *Nucleic*
544 *Acids Res.* **40**, D1100–D1107 (2011).
- 545 27. Wang, S., Witek, J., Landrum, G. A. & Riniker, S. Improving Conformer Generation for
546 Small Rings and Macrocycles Based on Distance Geometry and Experimental Torsional-
547 Angle Preferences. *J. Chem. Inf. Model.* **60**, 2044–2058 (2020).
- 548 28. Friedrich, N.-O. *et al.* High-Quality Dataset of Protein-Bound Ligand Conformations and

- 549 Its Application to Benchmarking Conformer Ensemble Generators. *J. Chem. Inf. Model.* **57**,
550 529–539 (2017).
- 551 29. Friedrich, N.-O. *et al.* Benchmarking Commercial Conformer Ensemble Generators. *J.*
552 *Chem. Inf. Model.* **57**, 2719–2728 (2017).
- 553 30. Cappel, D., Dixon, S. L., Sherman, W. & Duan, J. Exploring conformational search
554 protocols for ligand-based virtual screening and 3-D QSAR modeling. *J. Comput. Aided*
555 *Mol. Des.* **29**, 165–182 (2014).
- 556 31. Schreyer, A. M. & Blundell, T. USRCAT: real-time ultrafast shape recognition with
557 pharmacophoric constraints. *J. Cheminform.* **4**, (2012).
- 558 32. Bonanno, E. & Ebejer, J.-P. Applying Machine Learning to Ultrafast Shape Recognition in
559 Ligand-Based Virtual Screening. *Frontiers in Pharmacology* vol. 10 (2020).
- 560 33. Wójcikowski, M., Zielenkiewicz, P. & Siedlecki, P. Open Drug Discovery Toolkit (ODDT):
561 a new open-source player in the drug discovery field. *J. Cheminform.* **7**, 26 (2015).
- 562 34. Gladysz, R. *et al.* Spectrophores as one-dimensional descriptors calculated from three-
563 dimensional atomic properties: applications ranging from scaffold hopping to multi-target
564 virtual screening. *J. Cheminform.* **10**, 9 (2018).
- 565 35. Wang, Y. *et al.* TF3P: Three-Dimensional Force Fields Fingerprint Learned by Deep
566 Capsular Network. *J. Chem. Inf. Model.* **60**, 2754–2765 (2020).
- 567 36. ClinicalTrials.gov. <http://ClinicalTrials.gov>.
- 568 37. Chen, X. & Geiger, J. D. Janus sword actions of chloroquine and hydroxychloroquine
569 against COVID-19. *Cell. Signal.* **73**, 109706 (2020).
- 570 38. Frediansyah, A., Nainu, F., Dhama, K., Mudatsir, M. & Harapan, H. Remdesivir and its
571 antiviral activity against COVID-19: A systematic review. *Clin Epidemiol Glob Health*

- 572 (2020) doi:10.1016/j.cegh.2020.07.011.
- 573 39. Agrawal, U., Raju, R. & Udawadia, Z. F. Favipiravir: A new and emerging antiviral option
574 in COVID-19. *Armed Forces Med. J. India* **76**, 370–376 (2020).
- 575 40. Halgren, T. A. Merck molecular force field. I. Basis, form, scope, parameterization, and
576 performance of MMFF94. *Journal of Computational Chemistry* vol. 17 490–519 (1996).
- 577 41. MongoDB Atlas Database. <https://www.mongodb.com>.
- 578 42. Cortés-Cabrera, A., Morris, G. M., Finn, P. W., Morreale, A. & Gago, F. Comparison of
579 ultra-fast 2D and 3D ligand and target descriptors for side effect prediction and network
580 analysis in polypharmacology. *British Journal of Pharmacology* vol. 170 557–567 (2013).
- 581 43. <http://zinc15.docking.org/>. <http://zinc15.docking.org/>.
- 582 44. REAL Database - Enamine. [https://enamine.net/library-synthesis/real-compounds/real-](https://enamine.net/library-synthesis/real-compounds/real-database)
583 [database](https://enamine.net/library-synthesis/real-compounds/real-database).
- 584 45. Shirvaliloo, M. Targeting the SARS-CoV-2 3CLpro and NO/cGMP/PDE5 pathway in
585 COVID-19: a commentary on PDE5 inhibitors. *Future Cardiol.* (2021) doi:10.2217/fca-
586 2020-0201.
- 587 46. Jin, Z. *et al.* Structure of M pro from SARS-CoV-2 and discovery of its inhibitors. *Nature*
588 **582**, 289–293 (2020).
- 589 47. Vena, F. *et al.* MEK inhibition leads to BRCA2 downregulation and sensitization to DNA
590 damaging agents in pancreas and ovarian cancer models. *Oncotarget* **9**, 11592–11603
591 (2018).
- 592 48. Zhou, L. *et al.* MEK inhibitors reduce cellular expression of ACE2, pERK, pRb while
593 stimulating NK-mediated cytotoxicity and attenuating inflammatory cytokines relevant to
594 SARS-CoV-2 infection. *Oncotarget* **11**, 4201 (2020).

- 595 49. The MEK-inhibitor CI-1040 displays a broad anti-influenza virus activity in vitro and
596 provides a prolonged treatment window compared to standard of care in vivo. *Antiviral Res.*
597 **142**, 178–184 (2017).
- 598 50. Liu, S. *et al.* Potential Antiviral Target for SARS-CoV-2: A Key Early Responsive Kinase
599 during Viral Entry. *CCS Chemistry* 559–568 (2021) doi:10.31635/ccschem.021.202000603.
- 600 51. Olubiyi, O. O., Olagunju, M., Keutmann, M., Loschwitz, J. & Strodel, B. High Throughput
601 Virtual Screening to Discover Inhibitors of the Main Protease of the Coronavirus SARS-
602 CoV-2. *Molecules* **25**, 3193 (2020).
- 603 52. Kircheis, R. *et al.* NF- κ B Pathway as a Potential Target for Treatment of Critical Stage
604 COVID-19 Patients. *Front. Immunol.* **11**, (2020).
- 605 53. Hariharan, A., Hakeem, A. R., Radhakrishnan, S., Reddy, M. S. & Rela, M. The Role and
606 Therapeutic Potential of NF-kappa-B Pathway in Severe COVID-19 Patients.
607 *Inflammopharmacology* **1**.
- 608 54. Oxytocin activates NF- κ B-mediated inflammatory pathways in human gestational tissues.
609 *Mol. Cell. Endocrinol.* **403**, 64–77 (2015).
- 610 55. Hernández-Presa, M. *et al.* Angiotensin-converting enzyme inhibition prevents arterial
611 nuclear factor-kappa B activation, monocyte chemoattractant protein-1 expression, and
612 macrophage infiltration in a rabbit model of early accelerated atherosclerosis. *Circulation*
613 **95**, (1997).
- 614 56. Burzynski, L. C. *et al.* The Coagulation and Immune Systems Are Directly Linked through
615 the Activation of Interleukin-1 α by Thrombin. *Immunity* vol. 50 1033–1042.e6 (2019).
- 616 57. Ísis Venturi Biembengut, T. de A. C. B. de S. Coagulation modifiers targeting SARS-CoV-
617 2 main protease Mpro for COVID-19 treatment: an in silico approach. *Mem. Inst. Oswaldo*

- 618 *Cruz* **115**, (2020).
- 619 58. Optibrium. Optibrium - StarDrop: Nova - A new generation of possibilities.
620 <https://www.optibrium.com/stardrop/stardrop-nova.php>.
- 621 59. Gohda, K., Mori, I., Ohta, D. & Kikuchi, T. 10.1023/A:1008193217627. *Journal of*
622 *Computer-Aided Molecular Design* vol. 14 265–275 (2000).
- 623 60. Mackerell, A. D., Jr. Empirical force fields for biological macromolecules: overview and
624 issues. *J. Comput. Chem.* **25**, 1584–1604 (2004).
- 625 61. Hasegawa, K., Arakawa, M. & Funatsu, K. Rational choice of bioactive conformations
626 through use of conformation analysis and 3-way partial least squares modeling.
627 *Chemometrics Intellig. Lab. Syst.* **50**, 253–261 (2000).
- 628 62. Acharya, C., Coop, A., Polli, J. E. & Mackerell, A. D., Jr. Recent advances in ligand-based
629 drug design: relevance and utility of the conformationally sampled pharmacophore
630 approach. *Curr. Comput. Aided Drug Des.* **7**, 10–22 (2011).
- 631 63. Ullrich, S. & Nitsche, C. The SARS-CoV-2 main protease as drug target. *Bioorganic &*
632 *Medicinal Chemistry Letters* vol. 30 127377 (2020).
- 633 64. Elfiky, A. A. SARS-CoV-2 RNA dependent RNA polymerase (RdRp) targeting: an
634 perspective. *J. Biomol. Struct. Dyn.* 1–9 (2020).
- 635 65. Li, W. *et al.* Angiotensin-converting enzyme 2 is a functional receptor for the SARS
636 coronavirus. *Nature* vol. 426 450–454 (2003).
- 637 66. Vincent, M. J. *et al.* Chloroquine is a potent inhibitor of SARS coronavirus infection and
638 spread. *Viol. J.* **2**, 69 (2005).
- 639 67. Website. *github.com - Quantori repository* <https://github.com/quantori/MultiRef3D>.
- 640 68. Targeted Libraries. <https://enamine.net/hit-finding/focused-libraries/>.

